

## Adsorption of Acid Orange 8 Dye from Aqueous Solution Onto Unmodified and Modified Zeolites

Tharcila Colachite Rodrigues Bertolini\*, Raquel Reis Alcântara, Juliana de Carvalho Izidoro, Denise Alves Fungaro

Chemical and Environmental Center, Nuclear and Energy Research Institute, Av. Prof. Lineu Prestes, 2242, CEP 05508-000, São Paulo, Brazil.

Article history: Received: 14 July 2015; revised: 30 September 2015; accepted: 10 October 2015. Available online: 30 December 2015. DOI: <http://dx.doi.org/10.17807/orbital.v7i4.764>

**Abstract:** The adsorption of the acid dye Acid Orange 8 (AO8) onto unmodified and modified zeolites from coal fly ash and bottom ash was evaluated. The coal fly ash and bottom ash used in the synthesis of the zeolites by alkaline hydrothermal treatment were collected in the Thermoelectric Complex Jorge Lacerda, located in the Santa Catarina State, Brazil, the largest coal burning thermoelectric complex of Latin America. The modified zeolites were modified using the surfactant hexadecyltrimethylammonium bromide. The zeolitic materials were characterized predominantly as hydroxysodalite and NaX. The kinetics studies indicated that the adsorption followed the pseudo-second order kinetics. Linear and non-linear regression methods were used to determine the best fit of equilibrium data. The Freundlich model was better adjusted to the experimental data for all systems studied. The parameters of adsorption isotherms were used to predict the design of the equipment for performing adsorption discontinuous single stage.

**Keywords:** acid orange 8; coal fly ash; coal bottom ash; zeolite; modified zeolite; adsorption

### 1. INTRODUCTION

The textile industry worldwide plays an important role, both for its growth and the generation of waste. It is a fragmented industry, and presents complex process and is considered one of the most polluting.

A stage of the production of the textile industry involves spinning, weaving and/or knitting, processing and ennobling of yarns and fabrics and clothing. The steps that consume more water and thus generating the most effluents are the processing and ennobling.

Besides the high water consumption, the dyeing process uses large amounts of dyes, these being of various types. The azo dyes are the one most widely used. The synthetic dyes are complex compounds, which exhibit considerable structural diversity and are highly toxic. Present sulfur, naphthol, vat dyes, nitrates, acetic acid, surfactants, enzymes chromium compounds and metals such as copper, arsenic, lead, cadmium, mercury, nickel, cobalt and certain auxiliary chemicals [1, 2].

The azo dyes are composed of one or more azo

groups (-N=N-), in connection with phenyl and naphthol radical, which are substituted with some combinations of functional groups including: amino (-NH<sub>2</sub>), chlorine (Cl), hydroxyl (-OH), methyl (-CH<sub>3</sub>), nitro (-NO<sub>2</sub>) the sulfonic acid and sodium salts (-SO<sub>3</sub>Na) [3]. Most of the dyes belonging to this group is highly resistant to natural degradation and have toxic potential in different organisms [4, 5].

An azo dye widely used in the textile market is acid orange 8 (AO8). Its principal application is in leather and wool dyeing and paper coloration, which makes its wastes an important economic issue. The AO8 is a strong electrolyte, it is completely dissociated under the acid conditions used in the dyeing process [6].

There is not even a simple technique, which may be considered as one universal solution in wastewater treatment, the current trend is focused on the integration of multiple techniques, and these may be chemical, physical and biological [7].

Among the physical processes of treatment, adsorption is being studied and considered a superior alternative, for reasons of cost, efficiency, practicality

\*Corresponding author. E-mail: [thacolachite@yahoo.com.br](mailto:thacolachite@yahoo.com.br)

and ease of operation [2, 8].

The activated carbon remains the most widely studied adsorbent, and it has been found to for the removal of pollutants from wastewaters by adsorption [9]. The design and operation of the process is convenient, but this material has high cost. Therefore, efforts are directed towards developing low-cost alternative adsorbents.

The preparation of low-cost adsorbents from waste materials has several advantages, mainly of economic and environmental nature. A wide variety of low-cost adsorbents have been prepared from different materials utilizing industrial, biomass, and municipal wastes [2, 8-10].

The thermoelectric power stations produce a great quantity of residues from combustion of coal, and the same are being investigated as potential adsorbents for the removal of pollutants from wastewaters [9].

In Brazil, the coal used in power plants is pulverized and burned inside a boiler, producing bottom ash (15-20 wt.%) of the bulk solid combustion-by-products produced), which falls inside the boiler, and fly ash (80-85 wt.%) [11].

The fly ash is little used mainly including pozzolanic cement, paving, bricks. The bottom ash is previously disaggregated and transported to the settling ponds through pumping hydraulic [12, 13].

The inadequate disposal of residues from combustion of coal causes serious environmental problems. The ashes have toxic substances that may pollute the soil, surface water and groundwater through leaching. One way to reduce the environmental impact of these wastes is to expand its utilization. The recycling of the coal ash at a low cost adsorbent is an alternative and able to remove toxic substances from contaminated waters [14-18].

The coal ash can be converted into zeolites due to their high contents of silicon and aluminum, which are the structural elements of zeolites. The most common method involves a hydrothermal treatment with sodium hydroxide [19, 20].

The utilization of zeolite from coal fly ash as a useful adsorbent material for water treatment is due to its large specific surface area, cation exchange capacity, mechanical strength and low cost [21-27].

The zeolite has a good affinity toward inorganic pollutants, but little or no ability to remove organic pollutants. This is expected due to hydrophilic nature

and a net negative surface charge of zeolites. As is well known, the surface properties of zeolites may be greatly modified with cationic surfactant by simple ion-exchange reactions [28-30]. Generally, these surfactants are formed by long alkyl chains with a quaternary ammonium group at one end of the chain.

One of the most commonly used surfactants for zeolite surface modification is hexadecyltrimethylammonium bromide (HDTMA-Br). Depending on the coating conditions, HDTMA-Br may form monolayers or bi layers on the zeolite surface and more often, a patchy mono-layer and/or bi-layers form on the surface.

Also, surfactant-modified zeolite has been employed for removal of major categories of water contaminants [28]. Several studies reported the effective use of zeolite from fly ash for removing dye, but there are seldom publications about the dye adsorption using zeolite from bottom ash.

The aim of this work was to modify synthesized zeolite from coal fly ash and bottom ash with cationic surfactant quaternary ammonium namely hexadecyltrimethylammonium to study the removal of anionic dye Acid Orange 8 from aqueous solutions. Therefore, adsorption kinetics and isotherm studies were undertaken to determine the adsorbate removal rate and the maximum adsorption capacity of the zeolites.

## 2. MATERIAL AND METHODS

All chemicals used for experimental studies were of analytical grade. The Acid Orange dye (AO8; CI 15575;  $C_{17}H_{13}N_2NaO_4S$ ;  $364.35 \text{ g mol}^{-1}$ ) provided from Aldrich and considered as purity 65%. The chemical structure of AO8 is show in Figure 1. A stock solution of AO8 was prepared with deionized water (Millipore Milli-Q) and the solutions for adsorption tests were prepared by diluting it. Concentrations of the aqueous solutions of dye were monitored on UV/Visible spectrophotometer (Varian 1E).

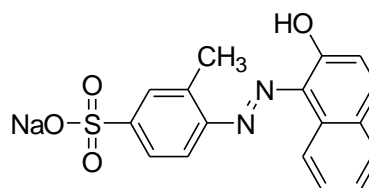


**Figure 1.** Chemical structure of Acid Orange 8.

The samples of coal fly (CFA) and bottom ashes

(CBA) were obtained from Jorge Lacerda coal-fired power plant located at Capivari de Baixo County, in Santa Catarina State, Brazil. The quaternary ammonium salt hexadecyltrimethylammonium bromide with molar mass  $364.46 \text{ g mol}^{-1}$  (HDTMA-Br, Merck) was used. The synthetic zeolite 4A in the form of balls company Bayer (ZBayer) was used in the study for comparison.

### Synthesis of zeolites from coal fly (ZFA) and bottom ashes (ZBA)

The zeolite was prepared by hydrothermal activation of 20 g of coal fly (CFA) or coal bottom ashes (CBA) at  $100 \text{ }^\circ\text{C}$  in 160 mL of  $3.5 \text{ mol L}^{-1}$  NaOH solution for 24 h. The zeolitic material was repeatedly washed with deionized water to remove excess sodium hydroxide until the washing water had pH  $\sim 10$ , then it was dried at  $50 \text{ }^\circ\text{C}$  for 12 h [31].

### Synthesis of modified zeolite from fly (MZSF) and bottom ash (MZSB)

The modified zeolite was prepared by mixing 10 g of ZFA or ZBA with 0.2 L of  $1.8 \text{ mmol L}^{-1}$  HDTMA-Br. The mixture of zeolite and HDTMA-Br solution was stirred for 7 h at 120 rpm and  $25 \text{ }^\circ\text{C}$ . The suspension was filtered and the solid was dried in oven at  $50 \text{ }^\circ\text{C}$  for 12 h.

### Characterization of Materials

The mineralogical compositions of the samples were determined by X-ray diffraction analyses (XRD) with an automated Rigaku multiflex diffractometer with Cu anode using Co  $K\alpha$  radiation at 40 kV and 20 mA over the range ( $2\theta$ ) of  $5\text{-}80^\circ$  with a scan time of  $0.5^\circ/\text{min}$ . The crystalline phases present in the samples were identified with the help of ICDD (International Centre for Diffraction Data). The chemical composition of materials was determined by X-ray fluorescence (XRF) in a Rigaku RIX- 3000 equipment.

For the cation exchange capacity (CEC) and external cation exchange capacity (ECEC) measurements, the samples were saturated with sodium acetate solution ( $1 \text{ mol L}^{-1}$ ), washed with 1L of distilled water and then mixed with ammonium acetate solution ( $1 \text{ mol L}^{-1}$ ) [32]. The sodium ion concentration of the resulting solution was determined by optical emission spectrometry with inductively coupled plasma - ICP-OES (Spectroflame - M120). The pH of zeolite was measured as follows: 0.1 g of samples were mixed with

10 mL of distilled water and shaken for 24 h. After filtration, the pH of solution was determined by a pH meter.

The determination of the point of zero charge ( $\text{pH}_{\text{PZC}}$ ) of samples was carried out as follows: the samples (0.1 g) were placed in 50 mL of potassium nitrate ( $0.1 \text{ mol L}^{-1}$ ) and the mixtures were stirred for 24 h in the mechanical stirrer (Quimis – MOD Q-225M) at 120 rpm. The initial pH values of solutions were adjusted to the values of 2, 4, 10, 11, 12 and 13 by addition of  $0.1$  and  $1 \text{ mol L}^{-1}$  HCl or  $3 \text{ mol L}^{-1}$  NaOH solution. The difference values between the initial and final pH ( $\text{pH } \Delta$ ) were placed in a graph in function of the initial pH. The point x where the curve intersects the  $y = 0$  is the  $\text{pH}_{\text{PZC}}$ .

The chemical composition and the some physicochemical properties of CFA and CBA have been described in a previous paper [22, 33].

### Adsorption studies

The adsorption for the adsorbents ZFA, ZBA, MZSF, MZSB and ZBayer was carried out in batch system (batch process) with aqueous solution of AO8.

The kinetic experiments were carried out by agitating of aliquots the dye solution with the adsorbents (with a mass / volume of  $0.01 \text{ mL g}^{-1}$ ) at 120 rpm for different time intervals (Table 1) at room temperature ( $25 \pm 2^\circ\text{C}$ ). The collected samples were then centrifuged and the concentration in the supernatant solution was analyzed using a UV spectrophotometer (Cary 1E, Varian) by measuring absorbance at  $\lambda = 488 \text{ nm}$ , which is the maximum of absorption of AO8.

**Table 1.** Concentration of AO8 and time interval in the adsorption kinetics study.

Adsorbent	Concentration ( $\text{mg L}^{-1}$ )	Time of agitation (min)
ZFA	2.0	10 -360
ZBA	2.0	60 - 1440
ZBayer	2.0	10 - 1440
MZSF	10.0	5 - 120
MZSB	10.0	5 - 300

The adsorption capacity ( $\text{mg g}^{-1}$ ) of adsorbents was calculated using equation 1:

$$q = \frac{V(C_0 - C_f)}{M} \quad (\text{equation 1})$$

where  $q$  is the adsorbed amount of dye per gram of adsorbent,  $C_0$  and  $C_f$  the concentrations of the dye in

the initial solution and equilibrium, respectively ( $\text{mg L}^{-1}$ );  $V$  the volume of the dye solution added (L) and  $M$  the amount of the adsorbent used (g).

The efficiency of adsorption (or removal) was calculated using the equation:

$$R = 100 \times \frac{(C_0 - C_f)}{C_0} \quad (\text{equation 2})$$

where  $R$  is the efficiency of adsorption (%),  $C_0$  is the initial concentration of dye ( $\text{mg L}^{-1}$ ),  $C_f$  is the equilibrium concentration of dye at time  $t$  ( $\text{mg L}^{-1}$ ).

The adsorption isotherms were carried out by agitating of adsorbents with AO8 (with a mass/volume of  $0.01 \text{ mL g}^{-1}$ ) over the concentration ranging from 1 at  $253 \text{ mg L}^{-1}$  till the equilibrium was achieved. The adsorption capacity ( $\text{mg g}^{-1}$ ) of adsorbents was calculated using the equation 1.

### Kinetic and Equilibrium Models

In order to investigate the adsorption processes of AO8 onto adsorbents, characteristic constants were determined using the linearized form of pseudo-first order (equation 3) and pseudo-second order (equation 4) and Elovich (equation 6) kinetic models with equations as follows:

$$\log_{10} (q_e - q) = \log_{10} q_e - k_1 t / 2.303 \quad (\text{equation 3})$$

$$\frac{1}{q_t} = \frac{1}{k_2 q_e^2} + \frac{t}{q_e} \quad (\text{equation 4})$$

where  $q_e$  is the amount of dye adsorbed at equilibrium ( $\text{mg g}^{-1}$ ),  $q_t$  is the amount of dye adsorbed at time  $t$  ( $\text{mg g}^{-1}$ ),  $k_1$  is the rate constant of the pseudo-first order adsorption ( $\text{min}^{-1}$ ), and  $k_2$  is the rate constant of the pseudo-second order kinetics ( $\text{g mg}^{-1} \text{ min}^{-1}$ ) [34-36]. The values of  $k_1$  and  $q_e$  were obtained from the slope and intercept respectively of plot of  $\log (q_e - q_t)$  versus  $t$  for pseudo-first order model. The values of  $q_e$  and  $k_2$  can be determined from the slope and intercept of a plot of  $t/q_t$  versus  $t$ , respectively for pseudo-second order model. The initial adsorption rate,  $h$  ( $\text{mg g}^{-1} \text{ min}^{-1}$ ), as  $t \rightarrow 0$  can be defined as (equation 5):

$$h = k_2 q_e^2 \quad (\text{equation 5})$$

where  $k_2$  is the rate constant of the pseudo-second order kinetics ( $\text{g mg}^{-1} \text{ min}^{-1}$ ) and  $q_e$  is the maximum adsorption capacity ( $\text{mg g}^{-1}$ ).

The model of the Elovich is satisfied in chemical adsorption processes and is suitable for systems with heterogeneous adsorbing surfaces [37].

The Elovich equation is given as follows [36, 38]:

$$q_t = \frac{1}{\beta} \ln(\alpha\beta) + \frac{1}{\beta} \ln(t) \quad (\text{equation 6})$$

where  $\alpha$  is the initial sorption rate ( $\text{mg g}^{-1} \text{ min}^{-1}$ ) and  $\beta$  is the desorption constant ( $\text{mg g}^{-1}$ ). Thus, the constants can be obtained from the slope and intercept of a straight line plot of  $q_t$  versus  $\ln t$ . The linearization of the equation giving the rate of reaction obtained the initial sorption rate,  $\alpha$  from the intercept of a straight line plot of  $q_t$  versus  $\ln t$ .

The equilibrium data obtained in the present study were analyzed using two different isotherm models, Langmuir (equation 7) and Freundlich (equation 8). The linear and nonlinear regression methods of analysis were used to evaluate various adsorption parameters. The mathematical equations of these models are presented below:

$$q_e = \frac{(Q_0 \cdot b_L \cdot C_e)}{(1 + b_L \cdot C_e)} \quad \text{or} \quad \frac{C_e}{q_e} = \frac{1}{Q_0 b_L} + \frac{C_e}{Q_0} \quad (\text{equation 7})$$

$$q_e = k_f \cdot (C_e)^{1/n} \quad \text{or} \quad \log(q_e) = \log(k_f) + \frac{1}{n} \log(C_e) \quad (\text{equation 8})$$

where  $C_e$  is the equilibrium concentration ( $\text{mg L}^{-1}$ ),  $q_e$  the amount adsorbed at equilibrium ( $\text{mg g}^{-1}$ ),  $Q_0$  is the maximum amount of adsorbate per unit weight of adsorbent to form a complete monolayer on the surface ( $\text{mg g}^{-1}$ );  $b$  is the Langmuir isotherm constant ( $\text{Lmg}^{-1}$ ), related to the affinity of the adsorption sites;  $k_f$  [ $(\text{mg g}^{-1}) (\text{Lmg}^{-1})^{1/n}$ ] and  $n$  are the Freundlich constants related to adsorption capacity and adsorption intensity of adsorbents, respectively.

In assessing the fit using linear analysis, the correlation coefficients are compared. The model that best fits the experimental data present value of  $R$  higher and closer to one. Besides the value of  $R$ , the Chi-square ( $\chi^2$ ) test was employed, the lowest values will be used to further validate the applicability of isotherms tested. This statistical analysis is based on the sum of the squares of the differences between the experimental and model calculated data, of which each

squared difference was divided by the corresponding data obtained by calculating from models [39]. The Chi-square ( $\chi^2$ ) can be represented by:

$$\chi^2 = \sum \frac{(q_{e \text{ exp}} - q_{e \text{ calc}})^2}{q_{e \text{ calc}}} \quad (\text{equation 9})$$

where  $q_{e \text{ exp}}$  is the equilibrium capacity of the adsorbent obtained from experiment ( $\text{mg g}^{-1}$ ), and  $q_{e \text{ calc}}$  is the equilibrium capacity obtained by calculating from the model ( $\text{mg g}^{-1}$ ).

### 3. RESULTS AND DISCUSSION

#### Characterization of the zeolitic materials

The X-ray diffractograms of unmodified zeolite, modified zeolite and modified zeolite saturated with dye obtained from coal fly ash and bottom ash are shown in Figures 2 and 3, respectively. The crystalline phases in all zeolitic materials were hydroxysodalite (JCPDS 31-1271) and NaX (JCPDS 38-0237) with peaks of quartz (JCPDS 85-0796) and mullite (JCPDS 74-4143) of ash that remained after the treatment. The mineralogical composition of ash used as raw material for the synthesis of zeolites depends on the geological factors related to the formation and deposition of coal and its combustion conditions.

The structural parameters of the modified zeolites are very close to that of corresponding parent zeolite, which indicate that the crystalline nature of the zeolites remained intact after modification treatment with HDTMA-Br.

It is also evident from the Figures 2-3 that there is no appreciable change in the spectra of adsorbents after AO8 molecules adsorption. The result suggests that when modified zeolitic materials get loaded by dye molecules the lattice structural not changed [40]. Some peaks for saturated zeolite have lower relative intensity than that for zeolite, which results from the adsorption of dye onto zeolite.

The chemical composition (as their stable oxides form) of the unmodified and modified zeolites was determined by X-ray fluorescence (XRF) is shown in Table 2. The main constituents of these adsorbents are silica ( $\text{SiO}_2$ ), alumina ( $\text{Al}_2\text{O}_3$ ), and ferric oxide ( $\text{Fe}_2\text{O}_3$ ). Quantities below 5 wt.% of  $\text{K}_2\text{O}$ ,  $\text{CaO}$ ,  $\text{TiO}_2$ ,  $\text{SO}_3$  and  $\text{MgO}$  are also observed. The presence of bromide in the MZSF and MZSB was detected since the positive charge of the cation HDTMA adsorbed on the zeolite surface is counterbalanced by anions

bromide. The  $\text{SiO}_2/\text{Al}_2\text{O}_3$  ratio for zeolites is associated to the cation exchange capacity [22]. The materials showed low values of the  $\text{SiO}_2/\text{Al}_2\text{O}_3$  ratio. In general, a low  $\text{SiO}_2/\text{Al}_2\text{O}_3$  ratio indicated a higher cation exchange.

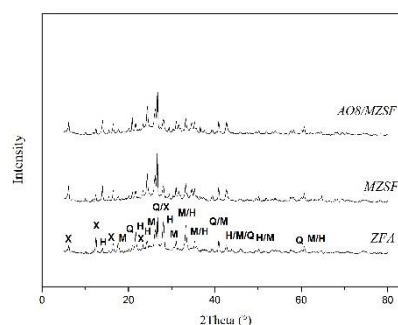


**Figure 2.** The X-ray diffraction patterns of the unmodified zeolite from fly ash; modified zeolite from fly ash before and after AO8 adsorption (Q = Quartz; M = Mullite; H = Hydroxysodalite zeolite, X = NaX zeolite).

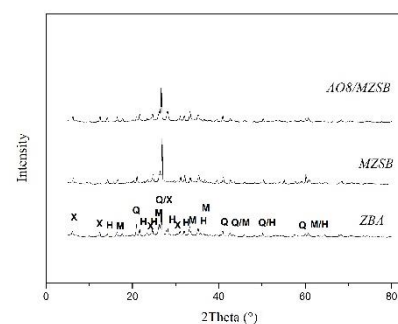


**Figure 3.** The X-ray diffraction patterns of the unmodified zeolite from bottom ash, modified zeolite from bottom ash before and after AO8 adsorption (Q = Quartz; M = Mullite; H = Hydroxysodalite zeolite, X = NaX zeolite).

**Table 2.** Chemical composition of the adsorbents.

Elements	ZFA	ZBA	MZSF	MZSB
$\text{Fe}_2\text{O}_3$	8.3	16.1	8.5	13
$\text{SiO}_2$	36.6	35.1	36	33
$\text{Al}_2\text{O}_3$	38	32.9	37	38
$\text{CaO}$	3.6	3.2	3.4	2.7
Br	-	-	0.06	0.05
$\text{TiO}_2$	2.7	2.4	2.7	2.0
$\text{SO}_3$	1.4	0.3	1.0	0.24
$\text{Na}_2\text{O}$	6.9	7.7	8.7	8.0
$\text{K}_2\text{O}$	0.8	0.7	0.8	0.7
$\text{ZnO}$	0.09	0.03	0.09	0.02
$\text{MgO}$	1.4	1.3	1.6	1.4
$\text{ZrO}_2$	0.05	0.04	0.06	0.04
$\text{SiO}_2/\text{Al}_2\text{O}_3$	0.96	1.06	0.97	0.87

Some physicochemical properties of zeolitic materials are given in Table 3. The CEC values

obtained for the unmodified and modified zeolites were very similar and varied between 1.19 e 1.61 meq g<sup>-1</sup>. CEC values of the zeolitic materials from fly ash were higher than bottom ash samples because CEC increase as the particle size of material becomes finer. The values of external cation exchange capacity (ECEC) of the adsorbents ZFA and ZBA obtained were lower than the CEC (13% and 12%, respectively). The large HDTMA<sup>+</sup> molecules do not have access to the internal surface and adsorb only to the external surface of zeolite. Consequently, ECEC characterizes the exchange capacity of the mineral surface for bulky surfactants and internal sites of the zeolite are still accessible to small ions [41].

**Table 3.** Physicochemical properties of the zeolitic materials.

	Zeolitic Materials			
	ZFA	MZSF	ZBA	MZSB
pH <sub>PZC</sub> <sup>a</sup>	6.5	6.3	7.3	6.1
CEC (meq g <sup>-1</sup> ) <sup>b</sup>	1.27	1.61	1.19	1.49
ECEC (meq g <sup>-1</sup> ) <sup>c</sup>	0.163	-	0.137	-
pH in water	8.4	8.3	8.4	8.5

(a) Point of zero charge; (b) cation exchange capacity; (c) external cation exchange capacity.

The values of the point zero charge (pH<sub>PZC</sub>) of

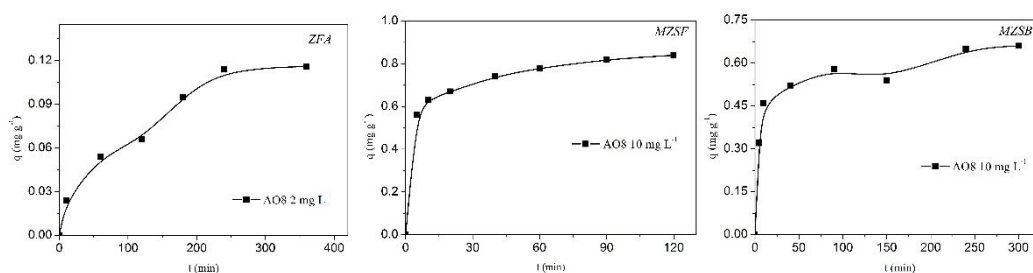


**Figure 4.** Effect of contact time on the adsorption of AO8 onto ZFA, MZSF and MZSB.

Table 4 presents a comparison between the kinetic data obtained at different zeolitic materials. The rapid removal of the dye and reach equilibrium in a short period of time is one of the indications that the adsorbent is efficiently and also allows the effluent treatment is more economical. As shown in Table 4, dye adsorption onto all the materials was very fast and the equilibrium was reached within 360 min for unmodified zeolite and between 90-240 min for modified zeolite. The organozeolites presented higher AO8 removal efficiency than the unmodified zeolite.

zeolites ZFA and ZBA (Table 3) were lower than pH in water indicating that the presented negative charge in aqueous solution (pH > pH<sub>PZC</sub>) for both adsorbents. The same occurred to MZSF and MZSB. Variations in the pH<sub>PZC</sub> values of adsorbents may be attributed to factors such as Si/Al ratio, the nature of crystallinity, impurity content, temperature, adsorption efficiency of electrolytes, degree of adsorption of H<sup>+</sup> and OH<sup>-</sup> [42].

In the case of modified adsorbent, among the factors that influence the pH<sub>PZC</sub> is also the concentration of surfactant used in surface modification. The change in relation to the pH<sub>PZC</sub> is related to the formations of monolayer or bilayer structure on the zeolite surface [43]. The negative charge of MZSF and MZSB indicated incomplete formation of bilayer of surfactant on the surface of zeolites.

### Adsorption Studies

The effect of the contact time in the adsorption of the AO8 on ZFA, ZBA, ZBayer, MZSF and MZSB was investigated. Representative concentration-time profiles for the sorption of AO8 dye on zeolitic materials are shown in Figure 4. The efficiency of dye removal was increased as the agitation time increased until equilibrium.

**Table 4.** Kinetics results for the adsorption of AO8 onto zeolitic materials.

Adsorbent	Initial Concentration (mg L <sup>-1</sup> )	Equilibrium time (min)	Removal (%)
ZFA	2.0	360	76
ZBA	2.0	--	zero
ZBayer	2.0	--	zero
MZSF	10.0	90	84
MZSB	10.0	240	68

For ZFB and ZBayer there was no removal of

the AO8 showing that the use of these adsorbents is not feasible for this dye under the conditions of this experimental study. This fact is not surprising due the large particle size of these materials. The adsorption efficiency increased with decreasing the particle size. The relatively higher adsorption with smaller adsorbent particle may be attributed to the fact that smaller particles yield large surface areas and the availability of more adsorption sites.

Previous studies have reported the little adsorption of AO8 onto unmodified zeolite from coal ash [44].

Aiming at evaluating the adsorption kinetics of AO8 onto adsorbents unmodified and modified, the pseudo-first order, pseudo-second order and Elovich kinetic models were used to fit the experimental data,

according to the kinetic model equations (3) to (6). The values of kinetic constants for AO8 adsorption onto adsorbents are presented in Table 5.

The quantitative evaluation of the models was performed by comparing the correlation coefficients (R). It can be seen from the data of Table 5 that R<sub>2</sub> correlation coefficients were greater than those of R<sub>1</sub> and R<sub>E</sub> for all dye/adsorbent systems. Hence, the pseudo-second order model better represented the adsorption kinetics. The mechanism of pseudo-second-order was also confirmed by comparing the values of q<sub>e</sub> determined experimentally (q<sub>e,exp</sub>) with the calculated q values (q<sub>e,calc</sub>) by the models (Table 5). The values of the calculated and experimental q<sub>e</sub> are close to the adsorbents.

**Table 5.** Kinetic parameters for AO8 removal onto ZFA, MZSF and MZSB.

Pseudo- first order						
Adsorbents	AO8 (mg L <sup>-1</sup> )	k <sub>1</sub> (min) <sup>-1</sup>	q <sub>e,calc</sub> (mg g <sup>-1</sup> )	q <sub>e,exp</sub> (mg g <sup>-1</sup> )	R <sub>1</sub>	
ZBA	2.0	1.52 x 10 <sup>-2</sup>	0.166	0.116	0.909	
MZSF	10.0	2.95 x 10 <sup>-2</sup>	0.310	0.840	0.996	
MZSB	10.0	1.21 x 10 <sup>-2</sup>	0.288	0.663	0.909	
Pseudo- second order						
		k <sub>2</sub> (g mg <sup>-1</sup> min <sup>-1</sup> )	h (mg g <sup>-1</sup> min <sup>-1</sup> )	q <sub>e,calc</sub> (mg g <sup>-1</sup> )	q <sub>e,exp</sub> (mg g <sup>-1</sup> )	R <sub>2</sub>
ZBA	2.0	7.83 x 10 <sup>-2</sup>	1.62 x 10 <sup>-3</sup>	0.144	0.116	0.970
MZSF	10.0	2.45 x 10 <sup>-1</sup>	1.81 x 10 <sup>-1</sup>	0.860	0.840	0.999
MZSB	10.0	1.31 x 10 <sup>-1</sup>	5.88 x 10 <sup>-2</sup>	0.666	0.663	0.995
Elovich						
		α (mg g <sup>-1</sup> min <sup>-1</sup> )	β (g mg <sup>-1</sup> )	R <sub>E</sub>		
ZBA	2.0	4.82 x 10 <sup>-3</sup>	37.2	0.952		
MZSF	10.0	14.7	12.0	0.993		
MZSB	10.0	2.43	14.2	0.946		

Table 5 presents the kinetic parameters obtained from the Elovich model fitted to experimental data. It was possible to observe that the initial adsorption rate (α) followed the order MZSF > MZSB, indicating that adsorption on modified zeolite from fly ash was faster than modified zeolite from bottom ash. Additionally, the value α for the modified zeolites was higher than for unmodified zeolite. This was in agreement with the trend observed in Figure 4. The parameter β is related to the extent of surface coverage present similar value for modified zeolite from fly and bottom ash.

### Adsorption Isotherm

The adsorption isotherms of the AO8 on ZFA, MZSF and MZSB are shown in Figures 5 and 6. The experimental values and curves achieved from the

values estimated by the Langmuir and Freundlich models from regressions linear and non-linear are presented.

The adsorption isotherm for solution may be classified into four main classes relating to their shapes termed S, L, H and C and subgroups 1, 2, 3, 4 or max. The equilibrium isotherms for the systems AO8/ZFA and AO8/MZSB showed curves corresponding to the class type L3, indicating a quick formation of a second adsorption layer. The curve presented in system AO8/MZSF have adapted to the type of class L4, indicating the formation of two layers, one on the first saturation of the adsorption surface and the other the new rear surface [45].

The linear regressive method of least squares is used for finding the parameters of the isotherms. The

relative parameters were obtained according to the intercept and slope from the linear plots. The non-linear regressive method of least sum squares of difference between calculated data and experimental

data was used to determine the isotherm parameters with OriginPro 8.0. The isotherm parameters from linear method and non-linear method were all listed in Table 6, respectively.

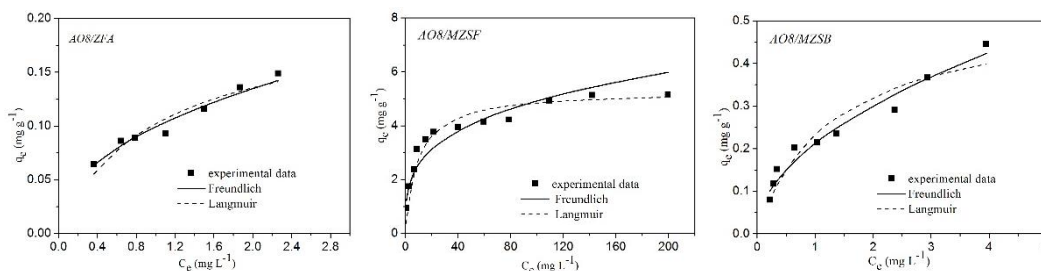


**Figure 5.** Adsorption isotherm of AO8 onto the adsorbents ( $T = 25 \pm 2$  °C) from the linear regression.

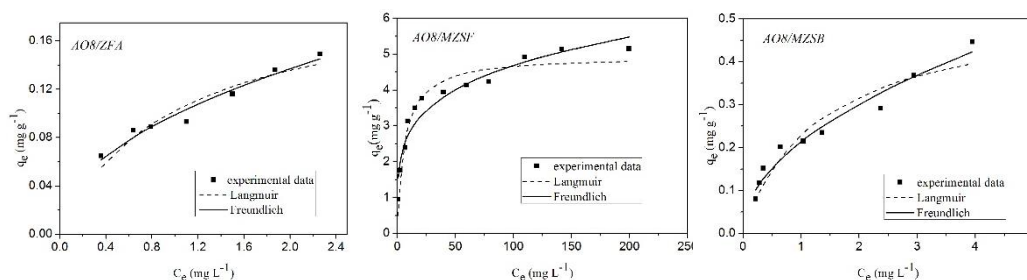


**Figure 6.** Adsorption isotherm of AO8 onto the adsorbents ( $T = 25 \pm 2$  °C) from the non-linear regression.

The Table 7 shows the values obtained of the test Chi-square ( $\chi^2$ ) and the correlation coefficients for each isotherm of dye systems/adsorbent obtained from linear and non-linear methods. When the two models are compared, from the linear regression, is observed

the largest correlation coefficient value (R) and the lowest values for  $\chi^2$ . For comparison of the models from the non-linear regression are considered the lowest values of deviation estimate (test Chi-square ( $\chi^2$ )).

**Table 2.** Langmuir and Freundlich isotherm parameters for AO8 adsorption on the adsorbents comparison of linear and non- linear methods.

Adsorbent	Parameters			
	Langmuir		Freundlich	
	$Q_0$ (mg g <sup>-1</sup> )	b	$k_f$ (mg g <sup>-1</sup> )(Lm g <sup>-1</sup> ) <sup>1/n</sup>	n
Linear method				
ZFA	0.20	1.06	$9.96 \times 10^{-2}$	2.28
MZSF	5.29	0.112	1.36	3.57
MZSB	0.522	0.820	0.214	2.01
Non-linear method				
ZFA	0.20	1.05	$9.92 \times 10^{-2}$	2.14
MZSF	4.94	0.167	1.68	4.48
MZSB	0.522	0.795	0.215	2.03

Although the Langmuir model has provided correlation coefficient values near to unit, lower values for  $\chi^2$  were observed in Freundlich equilibrium model both linear fit, as in the nonlinear adjustment. Thus, it was confirmed statistically that the Freundlich model was the best fit to the experimental data to describe the

system of the adsorption process under study.

The Freundlich isotherm constant, n, gives an idea for the favorability of the adsorption process. The value of n should be less than 10 and higher than unity for favorable adsorption conditions. As can be seen

from Table 6, the  $n$  values for the adsorbents were in the range of 1-10, indicating that the adsorption is a favorable process.

**Table 3.** Isotherm error deviation data related to the adsorption of AO8 onto the adsorbents.

Adsorbent	Models			
	Langmuir		Freundlich	
	R	$\chi^2$	R	$\chi^2$
Linear method				
ZFA	0.966	0.00489	0.981	0.00193
MZSF	0.997	1.414	0.962	0.614
MZSB	0.959	0.040	0.972	0.021
Non-linear method				
ZFA	-	0.00489	-	0.00193
MZSF	-	0.641	-	0.503
MZSB	-	0.043	-	0.021

As one was expected, the adsorbents originating from fly ash (ZFA and MZSF) exhibited higher maximum adsorption capacity compared to that originating from the bottom ash (MZSB). The variation in the adsorption can be explained by considering the differences in the granulometric characteristics (different particle sizes) of zeolitic materials as discussed in kinetic studies.

It is proposed that multiple mechanisms are involved in the adsorption of the AO8 on ZFA, MZSF and MZSB due to the wide variety of functional groups that its molecules have and surface properties of the adsorbents material.

The zeolitic materials have negative charge in water as demonstrated by determining the  $\text{pH}_{\text{PZC}}$  (Table 3). Unmodified zeolites have a net permanent negative charge resulting from isomorphous substitution of  $\text{Si}^{4+}$  by  $\text{Al}^{3+}$  in their crystal structures. Modified zeolite has a negative charge due the formation of incomplete of bilayer of surfactant on the surface.

The AO8 dye contains sulfonate group ( $-\text{SO}_3^-$ ) in its molecule and, therefore, is an anionic dye in aqueous solution. Thus, the electrostatic interaction does not occur in AO8/zeolite system.

For unmodified zeolite, probably the interactions that occur are bonds between active sites (Si-O and O-H) on adsorbent and the  $-\text{SO}_3^-$  and  $-\text{N}=\text{N}-$  groups of the dye [46].

For modified zeolites, the partition of the anionic AO8 dye within the group "tail" of the

hydrophobic surfactant molecule is the main mechanism involved in adsorption. The interaction between C or N of HTDMA molecule and the aromatic and sulfonic groups of AO8 is another possible mechanism of the adsorption [47, 48].

### Designing batch adsorption from equilibrium data

The adsorption isotherms can be used to predict the design of single stage batch adsorption systems [49, 50]. The schematic diagram is shown in Figure 7.

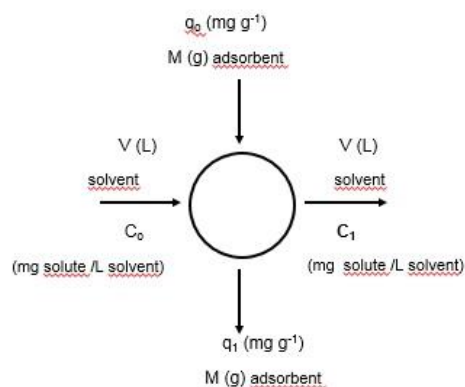


**Figure 7.** Schematic representation of the single stage batch adsorber system.

The design objective is to reduce the initial concentration  $C_0$  ( $\text{mg L}^{-1}$ ) of the dye solution volume  $V$  (L) to the concentration  $C_1$  ( $\text{mg L}^{-1}$ ). The amount of adsorbent is  $M$  (g) and the solute loading changes from  $q_0$  to  $q_1$  ( $\text{mg g}^{-1}$ ) adsorbent. At initial time ( $t = 0$ ),  $q_0 = 0$  and as time passes, the mass balance equates the dye removed from the liquid to that picked up by the solid. The mass balance equation of the adsorption system can be written as:

$$V(C_0 - C_1) = M(q_0 - q_1) = Mq_1 \quad (\text{equation 10})$$

If the system is allowed to come to equilibrium, then,

$$C_1 \rightarrow C_e \text{ and } q_1 \rightarrow q_e$$

Equation (10) can be rearranged as:

$$\frac{M}{V} = \frac{(C_0 - C_e)}{q_1} = \frac{C_0 - C_e}{q_e} = \frac{C_0 - C_e}{\frac{q_0 k_L C_e}{1 + k_L C_e}} \quad (\text{equation 11})$$

where  $q$  can be obtained by the equation of the isotherm that fit best to experimental data. In the example, is the Langmuir equation.

In this study, the isotherm model Freundlich

gives the best fit to experimental data. Therefore, the equation (8) can be applied for the calculation of  $q$ . A series of graphs for adsorption AO8 on the adsorbents synthesized in this work are shown in Figure 8. The initial concentrations of AO8 of 2 and 10 mg L<sup>-1</sup> were arbitrarily chosen for the purposes of the calculation of the quantities necessary of adsorbent to reduce the color (80, 85, 90 and 95% dye removal) in various

volumes of effluents. The concentration of 10 mg L<sup>-1</sup> is reported as the concentration found in real effluent [6].

According illustrates the Figure 8 (b), one can conclude that the amount of MZSF required to remove 90% of the AO8 will be 330, 397, 463, 529 g for volumes of 50, 60, 70 and 80 liters, respectively, for example.

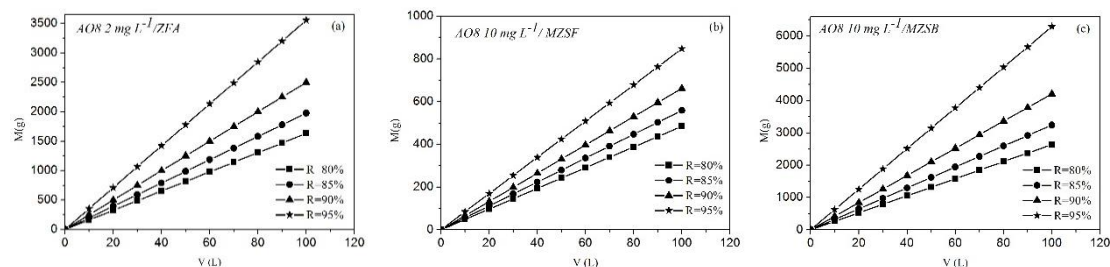


**Figure 8.** Adsorbent mass ratio with the volume of the treated solution; (a) AO8/ZFA; (b) AO8/MZSF; (c) AO8/MZSB.

The procedure is outlined in the adsorption system batch process of a single stage and may be modeled for other initial concentrations of the dyes, removal rates and volumes of effluent.

#### 4. CONCLUSION

This study investigated the equilibrium and the dynamics the adsorption of an anionic dye, which is namely Acid Orange 8 dye, AO8, onto unmodified zeolite (ZFA and ZBA) and modified zeolite (MZSF and MZSB) that were synthesized from coal fly and bottom ash, respectively. The X-ray diffraction analysis demonstrated that hydroxysodalite and NaX zeolites were formed after the synthesis. The pseudo-second order kinetic model agrees very well with the dynamic behavior for the adsorption of AO8 onto adsorbents. Linear and non-linear regressions were compared in this study to determine the preferred adsorption model. The Freundlich model was the most appropriate for fit of the equilibrium experimental data. It can be concluded from the results presented that materials based on modified zeolites from coal ash were effective as adsorbents for removal of Acid Orange 8 from water. The data from single-stage optimization models suggest that it will be useful for the design of adsorption plant for large-scale adsorption of Acid Orange 8 by MZSF from recycling streams.

#### 5. ACKNOWLEDGMENTS

The authors are grateful to Conselho Nacional de Desenvolvimento Científico e Tecnológico (CNPq), Coordenação de Aperfeiçoamento de Pessoal de Nível Superior (CAPES) for supporting this study and Jorge Lacerda coal-fired power plant for providing coal ash samples.

#### 6. REFERENCES AND NOTES

- [1] Carneiro, P. A.; Y.; Pupo Nogueira, R. F.; Zandoni, M. V. B. *Dye. Pigment.* **2007**, *74*, 127. [[CrossRef](#)]
- [2] Gupta, V. K.; Suhas. *J. Environ. Manage.* **2009**, *90*, 2013. [[CrossRef](#)]
- [3] Ventura-Camargo, B.C.; Marin-Morales, M. A. *Text. Light Ind. Sci. Tech.* **2013**, *2*, 85.
- [4] Guaratini, C. C. I.; Zandoni, M.V. *Quím. Nova.* **2000**, *23*, 71. [[CrossRef](#)]
- [5] Chequer, F. M. D.; Lizier, T. M.; Felício, R.; Zandoni, M. V. B.; Deboni, H.M.; Lopes, N.P.; Marcos, R.; Oliveira, D.P. *Toxicol. in Vitro* **2011**, *25*, 2054. [[CrossRef](#)]
- [6] Elizalde-González, M. P.; Garcia-Diaz, L. E. *Chem. Eng. J.* **2010**, *163*, 55. [[CrossRef](#)]
- [7] Kant, R. *Nat. Sci.* **2012**, *4*, 22. [[CrossRef](#)]
- [8] Ahmaruzzaman, M. *Adv. Colloid Interface Sci.* **2011**, *166*, 36.
- [9] Bhatnagar, A.; Sillanpaa, M. *Chem. Eng. J.* **2010**, *157*, 277. [[CrossRef](#)]
- [10] Gupta, V. K.; Carrott, P. J. M.; Ribeiro Carrott, M. M. L.; Suhas. *Crit. Rev. Env. Sci. Technol.* **2009**, *39*, 783.

- [CrossRef]
- [11] Depoi, F.S.; Pozebon, D.; Kalkreuth, W. D. *Int. J. Coal Geol.* **2008**, *76*, 227. [CrossRef]
- [12] Levandowski, J.; Kalkreuth, W. *Int. J. Coal Geol.* **2009**, *77*, 269. [CrossRef]
- [13] Cheriaf, M.; Péra, J., Rocha, J. C. *Cem. Concr. Res.* **1999**, *29*, 1387. [CrossRef]
- [14] Fungaro, D. A.; Silva, M. G. *Quím. Nova*, **2002**, *25*, 1081. [CrossRef]
- [15] Fungaro, D. A.; Flues, M. S. M.; Celebroni, A. P. *Quím. Nova*. **2004**, *27*, 582. [CrossRef]
- [16] Fungaro, D. A.; Izidoro, J. C.; Almeida, R. S. *Eclética Quím.* **2005**, *30*, 31. [CrossRef]
- [17] Fungaro, D. A.; Izidoro, J. C. *Tchê Quím.* **2006a**, *3*, 21.
- [18] Fungaro, D. A.; Izidoro, J.C. *Quím. Nova*. **2006b**, *29*, 735. [CrossRef]
- [19] Querol, X.; Moreno, N.; Umaña, J. C.; Alastuey, A.; Hernández, E.; López-Soler A.; Plana, F. *Int. J. Coal Geol.* **2002**, *50*, 413. [CrossRef]
- [20] Rayalu, S. S.; Bansawal, A. K.; Meshram, S. U.; Labhsetwar, N.; Devotta, S. *Catal. Sur. Asia*. **2006**, *10*, 74. [CrossRef]
- [21] Carvalho, T. E. M.; Fungaro, D. A.; Magdalena, C. P.; Cunico, P. J. *Radioanal. Nucl. Chem. Lett.* **2011**, *289*, 617. [CrossRef]
- [22] Izidoro, J. C.; Fungaro, D. A.; Santos, F. S.; Wang, S. *Fuel Process. Technol.* **2012**, *97*, 38. [CrossRef]
- [23] Izidoro, J. C.; Fungaro, D. A.; Abbott, J. E.; Wang, S. *Fuel*. **2012**, *103*, 82. [CrossRef]
- [24] Fungaro, D. A.; Bruno, M.; Grosche, L. C. *Desalin. Water Treat.* **2009**, *2*, 231. [CrossRef]
- [25] Fungaro, D. A.; Grosche, L. C.; Pinheiro, A. S.; Izidoro, J. C.; Borrelly, S. I. *Orbital Elec. J. Chem.* **2010**, *2*, 235. [Link]
- [26] Fungaro, D. A.; Yamaura, M.; Carvalho, T. E. M. *J. At. Mol. Sci.* **2011**, *2*, 305.
- [27] Fungaro, D. A.; Graciano, J. E. A. *Adsorpt. Sci. Technol.* **2007**, *10*, 729. [CrossRef]
- [28] Bowman, R.S. *Microporous Mesoporous Mater.* **2003**, *61*, 43. [CrossRef]
- [29] Haggerly, G.M.; Bowman, R.S. *Environ. Sci. Technol.* **1994**, *28*, 452. [CrossRef]
- [30] Li, Z.; Bowman, R. S. *Environ. Sci. Technol.* **1997**, *31*, 2407. [CrossRef]
- [31] Henmi, T. *Soil Sci. Plant Nutr.* **1987**, *33*, 517. [CrossRef]
- [32] Scott, J.; Guang, D.; Naeramitarnasuk, K.; Thabuot, M. J. *Chem. Technol. Biotechnol.* **2002**, *77*, 63. [CrossRef]
- [33] Bertolini, T. C. R.; Izidoro, J. C.; Magdalena, C. P.; Fungaro, D. A. *Orbital Elec. J. Chem.* **2013**, *5*, 179. [Link]
- [34] Blanchard, G.; Maunaye, M.; Martim, G. *Water Res.* **1984**, *18*, 1501. [CrossRef]
- [35] Ho, Y. S.; McKay, G. *Chem. Eng. J.* **1998**, *70*, 115. [CrossRef]
- [36] Ho, Y. S.; Mckay, G. *Process Biochem.* **1999**, *34*, 451. [CrossRef]
- [37] Aharoni, C.; Tompkins, F. C. In: Kinetics of adsorption and desorption and the Elovich equation. Eley, D. D.; Pines, H.; Weisz, P. B., eds. New York: Academic Press, 1970.
- [38] Sag, Y.; Aktay, Y. *Biochem. Eng. J.* **2002**, *12*, 143. [CrossRef]
- [39] Ho, Y. S. *Carbon*. **2004**, *42*, 2115. [CrossRef]
- [40] Lin, J.; Zhan, Y.; Zhu, Z.; Xing, Y. *J. Hazard. Mater.* **2011**, *193*, 102. [CrossRef]
- [41] Xie, J.; Meng, W.; Wu, D.; Zhang, Z.; Kong, H. *J. Hazard. Mater.* **2012**, *231*, 57. [CrossRef]
- [42] Fungaro, D. A.; Borrelly, S. I. *Ceram.* **2012**, *58*, 77. [CrossRef]
- [43] Li, Z. H.; Bowman, R. S. *Environ. Sci. Technol.* **1998**, *32*, 2278. [CrossRef]
- [44] Magdalena, C. P.; Fungaro, D. A. *Int. J. Adv. Res. Chem. Sci.* **2014**, *1*, 23.
- [45] Giles, C. H.; Macewan, T. H.; Nakhua, S. N.; Smith, D. J. *Chem. Soc.* **1960**, 3973. [CrossRef]
- [46] Acemioğlu, B. J. *Colloid Interface Sci.* **2004**, *274*, 371. [CrossRef]
- [47] Custelcean, R.; Jackson, J. E. *Chemical Reviews.* **2001**, *101*, 1963. [CrossRef]
- [48] Stefov, V.; Pejov, L.; Soptrajanov, B. *J. Mol. Struct.* **2003**, *649*, 231. [CrossRef]
- [49] Mckay, G.; Otterburn, M. S.; Aga, J. A. *Water Air Soil Pollut.* **1985**, *24*, 307. [CrossRef]
- [50] Özdemir, Y.; Dogan, M.; Alkan, M. *Microporous Mesoporous Mater.* **2006**, *96*, 419. [CrossRef]